Commentary

iMedPub Journals
http://www.imedpub.com

Biochemistry & Molecular Biology Journal
ISSN 2471-8084

2016
Vol. 2 No. 3: 17

DOI: 10.21767/2471-8084.100025

Three-Dimensional Architecture of the L-Type Calcium Channel: Structural Insights into the $Ca_V\alpha2\delta1$ Auxiliary Protein

Julie Briot[1,2,4], Nazzareno D'Avanzo[1,2], Jurgen Sygusch[2,3] and Lucie Parent[1,2,4]

1 Département de Physiologie Moléculaire et Intégrative, Faculté de Médecine, Canada
2 Groupe d'étude des Protéines membranaires, Canada
3 Département de Biochimie et Médecine Moléculaire, Faculté de Médecine, Université de Montréal, Montréal, Québec, Canada
4 Centre de Recherche de l'Institut de Cardiologie de Montréal, 5000 rue Bélanger, Montréal, Québec, Canada

Corresponding author:
Dr. Lucie Parent

lucie.parent@umontreal.ca

Département de Physiologie Moléculaire et Intégrative, Université de Montréal, Centre de Recherche de l'Institut de Cardiologie de Montréal, 5000 rue Bélanger, Montréal, Québec, H1T 1C8, Canada.

Tel: 514-343-6673

Abstract

L-type calcium channels (LTCC) are responsible for Ca^{2+} influx into muscle and neurons. These macromolecular complexes minimally comprise the main pore-forming $Ca_V\alpha1$ and auxiliary subunits $Ca_V\beta$ and $Ca_V\alpha2\delta1$. The ultrastructure of the oligomeric LTCC complexes from heart and skeletal muscle has been reported previously at ≈ 20 Å, a resolution that prevent identification of structural domains. Recent improvements in cryo-electronic microscopy (EM) methods made it possible to obtain a three-dimensional structure of the rabbit skeletal muscle LTCC $Ca_V1.1$ complex at a resolution of 4.2 Å and recently at 3.6 Å. This technique requires only nanograms of purified proteins and circumvents crystallization as a means for structure determination. The high resolution cryo-EM structure shows the molecular architecture of the subunits comprising the oligomeric complex and for the first time, a high-resolution glance of the largely extracellular $Ca_V\alpha2\delta1$ protein with its extracellular domains (Cache1, VWA, and Cache2). Although the $Ca_V\alpha2\delta1$ protein is a single-pass transmembrane protein, the complex topology of its extracellular domain represents a technical challenge for structure determination using conventional purification approaches. Herein we show the merits of a strategy based upon the purification of small structural domains that can be elucidated individually before these domains are reassembled into the quaternary structure. A structural model was derived using ab initio structure prediction constrained by small angle X-ray scattering profile of the refolded Cache2 domain. The excellent agreement between the predicted structure and the available cryo-EM structure suggests a novel and rapid procedure to discover structural information of protein domains.

Keywords: L-type calcium channel; Complexes architecture; $Ca_V\alpha2\delta1$ subunit; Electro-microscopy; Small angle X-ray scattering; Template-base modelling

Abbreviations: Cryo-EM: Cryo-Electron Microscopy; 3-D: Three Dimensional, PDB: Protein Data Bank; SAXS: Small Angle X-Ray Scattering; LTCC: L-Type Calcium Channel

Received: July 01, 2016; **Accepted:** September 18, 2016; **Published:** September 23, 2016

Citation: Briot J, D'Avanzo N, Sygusch J, et al. Three-Dimensional Architecture of the L-Type Calcium Channel: Structural Insights into the $Ca_V\alpha2\delta1$ Auxiliary Protein. Biochem Mol Biol J. 2016, 2:3.

Introduction

L-type calcium channels (LTCC) form a large family of structurally related channels expression in skeletal muscle ($Ca_V1.1$), working myocardium ($Ca_V1.2$), neuroendocrine cells ($Ca_V1.3$), and the retina ($Ca_V1.4$). In cardiac cells, calcium ions entering into the cell through $Ca_V1.2$ channels during the plateau phase of the action potential are essential to initiate the excitation-contraction coupling [1,2]. Together with voltage-gated sodium and potassium channels, $Ca_V1.2$ contributes to the heart rhythm and its activity can be derived from the measure of the QT interval on the electro cardiogram [3]. Gain-of-function and loss-of -function genetic mutations of sodium and potassium channels have been associated with many forms of cardiac arrhythmias [4]. To a smaller extent, mutations in the genes encoding for $Ca_V1.2$ channels have been associated with Timothy, Brugada, and early

after depolarization syndromes [5-7]. Some of these cardiac dysfunctions are characterized by an increase in the QT interval, whereas others are manifested by a shorter QT interval and an elevated ST segment [4,8].

In cardiomyocytes, $Ca_V1.2$ is an oligomer consisting of a main pore-forming $Ca_V\alpha1$ (≈ 250 kDa) and additional auxiliary subunits: $Ca_V\beta2$ (≈ 55 kDa) and $Ca_V\alpha2\delta1$ (≈ 150 kDa). The $Ca_V\alpha1$ subunit confers the biophysical and pharmacological properties of the channel and is the molecular target of the class IV antiarrhythmic drugs, among which dihydropyridine, verapamil, and diltiazem compounds are most widely used. This subunit is essential and targeted disruption of $Ca_V\alpha1$ is embryonically lethal in mice [9]. The intracellular $Ca_V\beta$ promotes cell surface trafficking of $Ca_V1.2$ through a nanomolecular interaction between the guanylate kinase domain of $Ca_V\beta$ and the hydrophobic residues of the α-helix formed in the cytoplasmic loop of the $Ca_V\alpha1$ subunit of $Ca_V1.2$ [10]. $Ca_V\alpha2\delta1$ increases peak current density and stabilizes the channel open state [6,11]. All three subunits are required to reproduce the biophysical properties of the native channel. Over the last 15 years, structural studies have revealed the high affinity interaction between $Ca_V\beta$ and $Ca_V\alpha1$ as well as the Ca^{2+}/calmoduline-$Ca_V\alpha1$ association by X-ray crystallography [12-15]. By contrast, there is little structural information on $Ca_V\alpha2\delta1$. The reason can be found in the complexity of the $Ca_V\alpha2\delta1$ protein topology that results from multiple co- and post-translational modifications including the addition of N-glycans at 16 Asn sites that is required for the folding and stability of $Ca_V\alpha2\delta1$ [16,17]. Furthermore, $Ca_V\alpha2\delta1$ is encoded by a single gene and is post-translationnally cleaved into the large extracellular $Ca_V\alpha2$ and the putative transmembrane $Ca_V\delta$ proteins bound by disulfide bridges [18-20]. In fact, the rat $Ca_V\alpha2\delta1$ protein includes 20 cysteine residues and it has been proposed that intra-molecular disulfide bonds are required to stabilize its higher order structure [21]. These features represent significant hurdles for expressing and purifying the protein complex in bacterial systems and account for the limited structural information on eukaryotic LTCC channels.

Three-Dimensional Structure of the Mammalian $Ca_V\alpha2\delta1$ Proteins

Structural data on the pore-forming subunit $Ca_V\alpha1$ has been mostly inferred from the high-resolution crystal structures (≈ 2.7 – 3.1 Å) of bacterial homologs of voltage-gated sodium channels and a modified variant referred to as Ca^{2+}-selective Ca_VAb channels [22-24]. Unlike their mammalian homologues, the bacterial channels form symmetrical channels with 4 identical subunits forming the pore region and appear to be functional without specific auxiliary subunits. Low-resolution electron microscopic (EM) models of the LTCC complex purified from skeletal muscle at a concentration of 90-140 µg LTCC complex for 400 g of skeletal muscle were first solved at 27 Å in 2004 [25]. The relatively low resolution provided a general outline of the protein complex and confirmed that $Ca_V\alpha2$ was mostly extracellular. More recently improvements in the electron detection and image processing algorithms made it possible to reconstruct the 3-D structure of the endogenous $Ca_V1.1$ channel complex from rabbit skeletal muscle membranes [17] without the need to obtain crystals. Instead of photoaffinity-labeling the protein complex with radioactive dihydropyridine receptor ligands [26], the authors chose the brilliant strategy to overexpress the cytosolic $Ca_V\beta1a$ subunit as a fusion protein in a bacterial system and use it as a bait to pull down with nanomolar affinity the entire LTCC complex [17,27]. Aliquots (4 µl) of the digitonin-purified $Ca_V1.1$ complex at 0.1 mg/ml were examined by cryo-EM and more than 10^6 particles were selected for further analysis. A three-dimensional structure of the LTCC complex with dimension of 170 x 100 Å was obtained at 4.2 Å [17] and then at 3.6 Å in the presence of 10 mM Ca^{2+} [27]. The electron density map revealed the position of the three subunits ($Ca_V\beta1a$, $Ca_V\gamma1$, and $Ca_V\alpha2\delta1$) in relation to the pore-forming $Ca_V\alpha1$ subunit of the $Ca_V1.1$ complex. In particular, the 3-D structure demonstrates for the first time the position of the transmembrane $Ca_V\gamma1$ protein, which is the major isoform expressed in the skeletal muscle [28]. More importantly, the authors provide the first description of the extracellular structural domains within $Ca_V\alpha2\delta1$ and their position relative to $Ca_V\alpha1$.

A BLASTP search conducted with the "conserved domain" tool in NCBI [29] revealed four structural domains in the extracellular region of the rabbit (NP_001075745.1) and the rat (NP_037051.2) $Ca_V\alpha2\delta1$ proteins: i.e., VWA-N, VWA, Cache2, and VGCC, the latter being included in the Cache2 domain identified in the cryo-EM structure of the rabbit $Ca_V\alpha2\delta1$ **(Figure 1)**. The VWA domain, believed to be the molecular target of anti-epileptic drugs of the gabapentin family [30], appears to be positioned just above the voltage sensor of the $Ca_V\alpha1$ subunit suggesting that $Ca_V\alpha2\delta1$ could modulate the channel function by stabilizing the channel voltage sensor domain [31]. There was however insufficient electron density to support amino acid assignment for the region between amino acids 627 to 950 within the unstructured C-terminal domain of $Ca_V\alpha2$ as well as for the $Ca_V\delta$ transmembrane domain between 1065 and 1106 in the first structure at 4.2 Å. Unfortunately, this relatively low resolution precluded assignment of the side chains even in regions where the backbone has been solved confidently such as in the N-terminal of $Ca_V\alpha2$ (between 40 and 77 and between 112 and 178).

The Cache domains face the extracellular environment and projects approximately 60 Å away from the membrane where it could anchor an extracellular networking hub for LTCC. Structural information could help identify crucial partners for protein trafficking and/or function [32]. Few mammalian homologs of the Cache2 domain are known. The primary sequence of the rat Cache2 domain of $Ca_V\alpha2\delta1$ share 24% and 34% identity in their primary sequences with the sensor domain of the *Bacillus subtillis* histidine kinase KinD (NP_389249.1) and the Cache domain of the methyl-accepting chemotaxis protein from *Methanosarcina mazei* (GI:295789445) respectively according to the local alignment search tool (blast) from the PDB database [33]. This relatively low homology and the small number of templates highlight the challenges of elucidating the three-dimensional structure of the $Ca_V\alpha2\delta1$ protein. The latter might prove to be a slightly superior template because the Cache domain of methyl-accepting chemotaxis protein possesses the same number of residues as the Cache2 domain of the rat $Ca_V\alpha2\delta1$ protein thus introducing no gap in the alignment. This contrasts with a gap

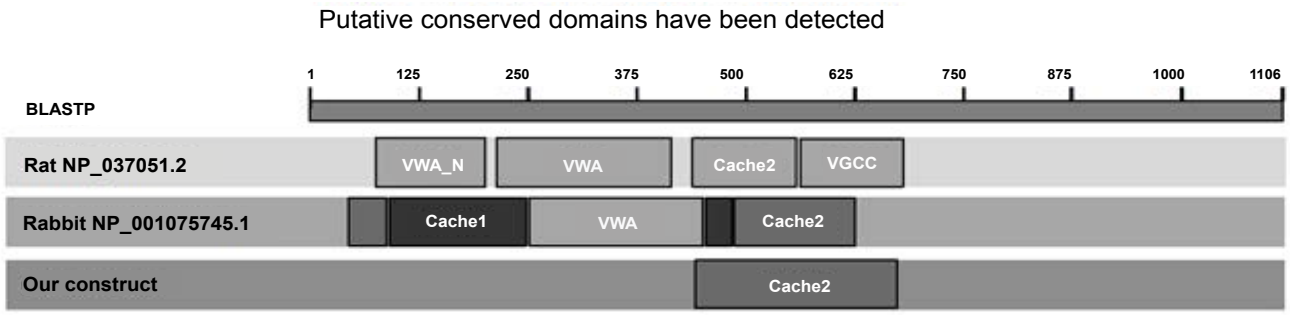

Figure 1 Typical conserved domains of voltage-gated calcium channel $Ca_V\alpha2\delta1$ subunit from *Rattus norvegicus* were identified by the NCBI Conserved Domain Search Database (http://blast.ncbi.nlm.nih.gov/Blast.cgi). For the rat $Ca_V\alpha2\delta1$ protein, the structural domains and the associated residues are: VWA_N (104-223), VWA (239-417), Cache2 (446-531), VGCC (543-636). For the rabbit $Ca_V\alpha2\delta1$ protein, the structural domains and the associated residues are: Cache1 (92-250; 444-484), VWA (251-443), Cache2 (76-91; 485-626). The overall primary sequence identity between the rat and the rabbit $Ca_V\alpha2\delta1$ proteins is 93.3%. Our construct goes from residue 446 to residue 636 and is referred to herein as Cache2.

of 11 residues with the former protein which accounts in part for the lower sequence identity. The online server I-TASSER [34-36] nonetheless confirmed these two proteins as the most appropriate templates for Cache2 domain of $Ca_V\alpha2\delta1$ suggesting that these proteins may share similar folding patterns.

The structural complexity of $Ca_V\alpha2\delta$ (disulfide bonds, multiple glycosylation sites, and one transmembrane domain) makes purification of the whole protein in a bacterial system quite challenging. To bypass these limitations, we implemented the "Divide and Conquer" approach [37] whereby the Cache2 domain, one of the basic building units of $Ca_V\alpha2\delta1$ [38], was cloned into a bacterial expression vector and purified for structure determination.

SAXS Structure of the Cache2 Domain of $Ca_V\alpha2\delta1$

The primary sequence of the rat Cache2 domains (between residues 446 and 636) display 93% identity with the rabbit isoform (between residues 448 and 651) (Figure 1). However, the rabbit Cache2 domain in the cryo-EM structure includes residues numbered 76 to 91 that are absent in our protein [38]. We overexpressed the Cache2 protein (rat residues 446-636) as a 25-kDa (HIS)6-tagged protein in *E. coli* BL21(DE3)pLYS. The protein was purified using a three-step purification procedure including affinity, DEAE and size exclusion chromatography. Most of the expressed protein found in inclusion bodies, was solubilized using 8 M urea and purified under denaturing conditions by immobilized metal ion affinity chromatography (IMAC) using a nickel resin followed by diethylaminoethanol anion-exchange chromatography. Refolding was achieved by removing urea by overnight dialysis at 4°C in the presence of 0.5 M of L-arginine, a stabilizing agent [39] and 1 mM DTT [40]. The Cache2 protein eluted as a single symmetric peak at 15.9 ml thus having an apparent molecular weight of 21 kDa according to our gel filtration calibrations. This validated the monomeric state of the purified Cache2 protein. The secondary structure of the purified domain contained 8% alpha helix and 41% beta strands. The protein was stable at 4°C at a pH of 7.4 for up to 2 weeks although N-glycosylation of eukaryotic proteins is generally not adequately performed in bacteria [41].

Structural characterization of the rat Cache2 protein was carried out using SAXS (small angle X-ray scattering) to assess the authenticity of the structure of the refolded protein. SAXS is a powerful method that provides structural information of proteins in solution [42], and requires small volumes (20-50 µl) of sample at relatively low protein concentration (0.1-1 mg/ml). SAXS provides information as to the folded/unfolded state of a protein, its aggregation, flexible domains, oligomeric state, shape and limited conformational data without any mass limitation [43]. When combined with biochemical knowledge and/or known atomic structures of component domains, SAXS provides an overall solution structure using flexible linkers to connect the structural domains [44] thus delivering a first approximation of the molecular shape, protein assembly and structural dynamics of biological macromolecules in their native state [44-46]. The program SAXSTER [47], an on-line service of the I-TASSER server, was used to build an *ab initio* model structure using the amino acid sequence of the rat Cache2 domain and was combined with the SAXS data as a constraint. The resulting model was then assessed against the coordinates of the Cache2 domain identified in the $Ca_V\alpha2\delta$ EM structure. SAXS data were collected on the refolded rat Cache2 protein at protein concentrations of 3.2, 1.6, 0.8 and 0.4 mg /ml **(Figure 2)**. The data collected at 3.2 mg /ml showed evidence of protein-protein interactions at very small angles and were thus excluded from further analysis. The Guinier plots (lnI(q) versus q^2) were linear for the remaining concentrations at very small scattering angle ($q*R_g<1.3$) indicative of sample monodispersity. The *ab initio* molecular envelopes of the rat Cache2 protein were reconstructed and averaged in DAMMIN [48]. The resulting envelope was bean-shaped and slightly asymmetrical (Figure 2) with dimensions of 71× 51× 20 Å corresponding to the D_{max} of 70 Å obtained from the pair distance probability plot [49]. The atomic coordinates of the rabbit Cache2 domain (rabbit amino acids from 448 to 651) were superimposed onto the experimental envelope using SUPCOMB program. CRYSOL was then used to calculate the solution scattering of the atomic structure of the rabbit Cache2 which was then used to fit

our experimental SAXS data [50]. The discrepancy was evaluated with a chi-square value of 1.14 (Figure 3A). The analysis was performed using a Cache2 model from SAXSTER and when superimposed onto the experimental envelope, an improved chi-square value of 1.05 as illustrated by comparing panels A and B in **Figure 3**.

The refolded rat structure is shown to superimpose well with the rabbit EM with a Root Mean Square Deviation for C-alpha carbons = 1.73 Å **(Figure 4)**. In particular, the structured N-terminal β-strands 1 and 2 as well as the α-helix 1 and 2 located downstream display the best fits. The "cores" of the rabbit Cache2 and the rat Cache2 proteins are identical. Structural differences occur in the intervening loop between the amino acids 532 and 551 of the rabbit Cache2 and the rat Cache2 proteins presumably due to differences in the primary sequence between the two isoforms and due to seven additional amino acids in the primary sequence of the rat Cache2 a C-terminus a TEV cleavage site, and 6 histidine residues. The SAXS envelope from the rat Cache2 refolded protein was also well fitted by the molecular coordinates of the KinD/methyl-accepting chemotaxis protein and consistent with an ambiguous score of 2.3 obtained when performing the AMBIMETER calculation [51].

Conclusion

$Ca_v\alpha2\delta1$ is an integrin-like protein that belongs to the LTCC complex. It promotes LTCC activation and as a result it enhances heart contractility [11]. $Ca_v\alpha2\delta1$ undergoes many co- and post-translational modifications that create a sizable challenge for its purification. In this short commentary, we have shown that the Cache2 domain of $Ca_v\alpha2\delta1$ can be purified and refolded from bacterial cultures at a yield of 2 mg per liter. SAXS data measured for the refolded protein enabled an *ab initio* prediction of a model structural whose fold was identical to the native state. The refolded Cache2 protein conserved the overall folding of the Cache2 protein purified from rabbit skeletal muscle, even though $Ca_v\alpha2\delta1$ exists mostly as a large extracellular domain loosely organized around multiple β-sheets [52]. Altogether, this validates an experimental strategy based upon the purification of isolated domains of LTCC subunits in a bacterial system and paves the way for implementing a "building block" approach in studying the structural biology of complex membrane proteins.

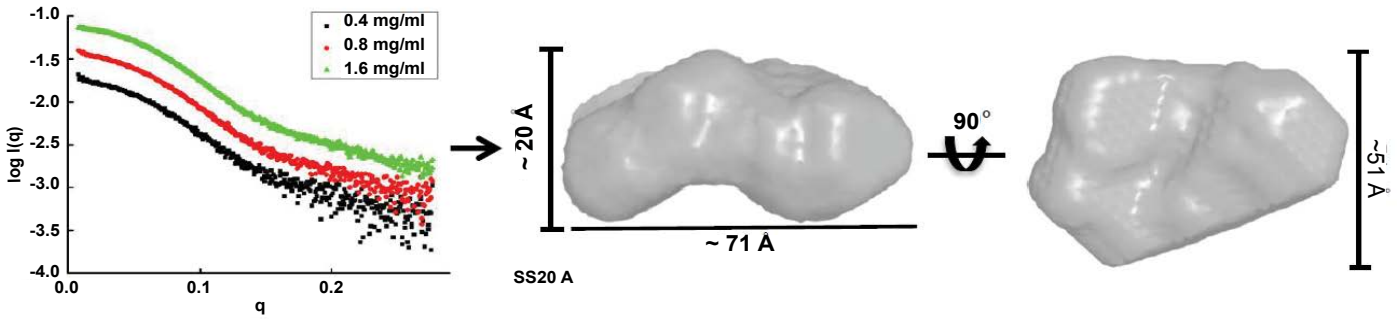

Figure 2 SAXS intensity profile of the rat Cache2 protein obtained for three different concentrations (0.4 mg/ml, 0.8 mg/ml, 1.6 mg/ml). Experimental SAXS data was used to build a low-resolution envelope of Cache2 using DAMMIN. The envelope dimensions are shown below.

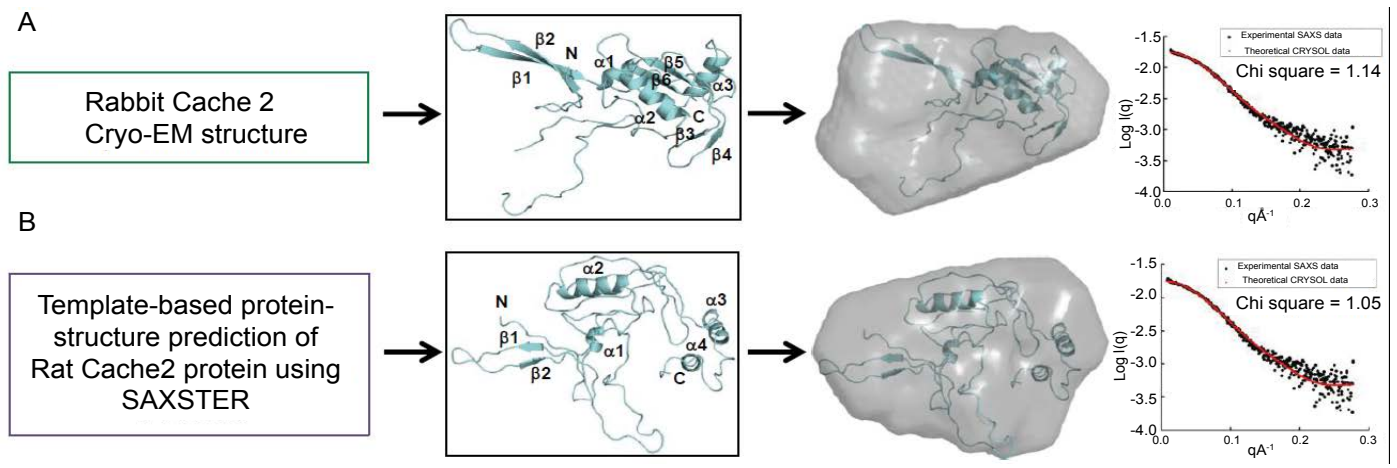

Figure 3 (A) The Rabbit Cache2 structure obtained from the of the Cryo-EM structure of the voltage-gated calcium channel (pdb code: 3JBR_F) was superimposed using SUPCOMB program with the experimental Cache2 envelope. As seen, the two curves deviated only slightly with a chi-square of 1.14. (B) The SAXTER Rat Cache2 model was superimposed with the experimental envelope of Cache2. The two curves agree with a chi-square of 1.05.

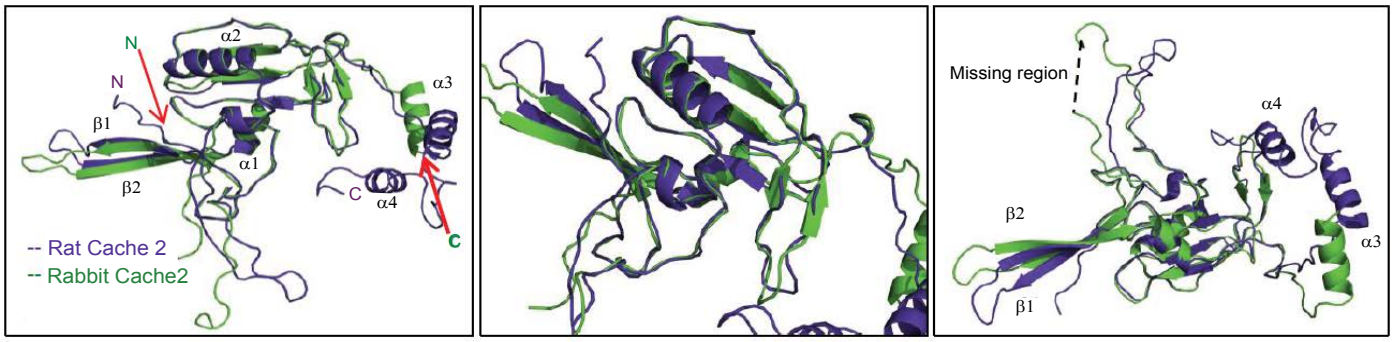

Figure 4 The refolded Rat Cache2 model (colored in violet) was superposed with the atomic coordinates of the Rabbit Cache2 domain (colored in green) in PyMOL.

Acknowledgments

We thank Dr. Christian Baron, from the Department de "Biochimie et Médecine Moléculaire", and Bastien Casu, Ph.D. student. This work was supported by a "Discovery" grant 262048-2012 from the Natural Sciences and Engineering Research Council of Canada to LP.

This work is based upon research conducted at the Cornell High Energy Synchrotron Source (CHESS), which is supported by the National Science Foundation and the National Institutes of Health/National Institute of General Medical Sciences under NSF award DMR-0936384, using the Macromolecular Diffraction at CHESS (MacCHESS) facility, which is supported by award GM-103485 from the National Institutes of Health, through its National Institute of General Medical Sciences.

References

1 Catterall WA (2011) Voltage-gated calcium channels. Cold Spring Harb Perspect Biol 3: a003947.

2 Shaw RM, Colecraft HM (2013) L-type calcium channel targeting and local signalling in cardiac myocytes. Cardiovasc Res 98: 177-186.

3 Moss AJ, Kass RS, Long QT (2005) syndrome: from channels to cardiac arrhythmias. J Clin Invest 115: 2018-2024.

4 Napolitano C, Antzelevitch C (2011) Phenotypical manifestations of mutations in the genes encoding subunits of the cardiac voltage-dependent L-type calcium channel. Circulation research 108: 607-618.

5 Burashnikov E, Pfeiffer R, Barajas-Martinez H, Delpon E, Hu D, et al. (2010) Mutations in the cardiac L-type calcium channel associated with inherited J-wave syndromes and sudden cardiac death. HeartRhythm 7: 1872-1882.

6 Bourdin B, Shakeri B, Tetreault MP, Sauve R, Lesage S, et al. (2015) Functional characterization of Ca_Valpha2delta mutations associated with sudden cardiac death. J Biol Chem 290: 2854-2869.

7 Raybaud A, Dodier Y, Bissonnette P, Simoes M, Bichet DG, et al. (2006) The role of the GX9GX3G motif in the gating of high voltage-activated Ca2+ channels. J Biol Chem 281: 39424-39436.

8 Fukuyama M, Ohno S, Wang Q, Kimura H, Makiyama T, et al. (2013) L-type calcium channel mutations in Japanese patients with inherited arrhythmias. Circulation 77: 1799-1806.

9 Rosati B, Yan Q, Lee MS, Liou SR, Ingalls B, et al. (2011) Robust L-type calcium current expression following heterozygous knockout of the Ca_V1.2 gene in adult mouse heart. J Physiol 589: 3275-3288.

10 Bourdin B, Marger F, Wall-Lacelle S, Schneider T, Klein H, et al. (2010) Molecular determinants of the Ca_Vbeta-induced plasma membrane targeting of the Ca_V1.2 channel. J Biol Chem 285: 22853-22863.

11 Fuller-Bicer GA, Varadi G, Koch SE, Ishii M, Bodi I, et al. (2009) Targeted disruption of the voltage-dependent calcium channel alpha2/delta -1-subunit. Am J Physiol Heart Circ Physiol 297: H117-H124.

12 Van Petegem F, Clark KA, Chatelain FC, Minor Jr DL (2004) Structure of a complex between a voltage-gated calcium channel beta-subunit and an alpha-subunit domain. Nature 429: 671-675.

13 Van Petegem F, Chatelain FC, Minor Jr DL (2005) Insights into voltage-gated calcium channel regulation from the structure of the Ca_V1.2 IQ domain-Ca2+/calmodulin complex. Nature structural & molecular biology 12: 1108-1115.

14 Chen YH, Li MH, Zhang Y, He LL, Yamada Y, et al. (2004) Structural basis of the alpha1-beta subunit interaction of voltage-gated Ca2+ channels. Nature 429: 675-680.

15 Opatowsky Y, Chen CC, Campbell KP, Hirsch JA (2004) Structural analysis of the voltage-dependent calcium channel beta subunit functional core and its complex with the alpha 1 interaction domain. Neuron 42: 387-399.

16 Tetreault MP, Bourdin B, Briot J, Segura E, Lesage S, et al. (2016) Identification of Glycosylation Sites Essential for Surface Expression of the Ca_Valpha2delta1 Subunit and Modulation of the Cardiac Ca_V1.2 Channel Activity. J Biol Chem 291: 4826-4843.

17 Wu J, Yan Z, Li Z, Yan C, Lu S, et al. (2015) Structure of the voltage -gated calcium channel Ca_V1.1 complex. Science 350: 2395.

18 Dolphin AC (2013) The alpha2delta subunits of voltage-gated calcium channels. Biochim Biophys Acta 1828: 1541-1549.

19 Douglas L, Davies A, Wratten J, Dolphin AC (2006) Do voltage-gated calcium channel alpha2delta subunits require proteolytic processing into alpha2 and delta to be functional? Biochem Soc Trans 34: 894-898.

20 Davies A, Kadurin I, Alvarez-Laviada A, Douglas L, Nieto-Rostro M, et al. (2010) The alpha2delta subunits of voltage-gated calcium channels form GPI-anchored proteins, a posttranslational modification essential for function. Proc Natl Acad Sci USA 107: 1654-1659.

21 Klugbauer N, Marais E, Hofmann F (2003) Calcium channel alpha2delta subunits: differential expression, function, and drug binding. J Bioenerg Biomembr 35: 639-647.

22 Catterall WA, Swanson TM (2015) Structural Basis for Pharmacology of Voltage-Gated Sodium and Calcium Channels. Mol Pharmacol 88: 141-150.

23 Payandeh J, Scheuer T, Zheng N, Catterall WA (2011) The crystal structure of a voltage-gated sodium channel. Nature 475: 353-358.

24 Tang L, Gamal El-Din TM, Payandeh J, Martinez GQ, Heard TM, et al. (2014) Structural basis for Ca2+ selectivity of a voltage-gated calcium channel. Nature 505: 56-61.

25 Wang MC, Collins RF, Ford RC, Berrow NS, Dolphin AC, et al. (2004) The three-dimensional structure of the cardiac L-type voltage-gated calcium channel: comparison with the skeletal muscle form reveals a common architectural motif. J Biol Chem 279: 7159-7168.

26 Sharp AH, Imagawa T, Leung AT, Campbell KP (1987) Identification and characterization of the dihydropyridine-binding subunit of the skeletal muscle dihydropyridine receptor. J Biol Chem 262: 12309-12315.

27 Wu J, Yan Z, Li Z, Qian X, Lu S, et al. (2016) Structure of the voltage-gated calcium channel Ca_V1.1 at 3.6 A resolution. Nature 537: 191-196.

28 Jay SD, SB Ellis, McCue AF, Williams ME, Vedvick TS, et al. (1990) Primary structure of the gamma subunit of the DHP-sensitive calcium channel from skeletal muscle. Science 248: 490-492.

29 Marchler-Bauer A, Derbyshire MK, Gonzales NR, Lu SN, Chitsaz F, et al. (2015) Cdd: Ncbi's Conserved Domain Database. Nucleic Acids Res 43: D222-D226.

30 Savalli N, Pantazis A, Sigg D, Weiss JN, Neely A, et al. (2016) The alpha2delta-1 subunit remodels Ca_V1.2 voltage sensors and allows Ca2+ influx at physiological membrane potentials. J Gen Physiol 148: 147-159.

31 Minor Jr DL, Findeisen F (2010) Progress in the structural understanding of voltage-gated calcium channel (Ca_V) function and modulation. Channels 4: 459-474.

32 Brown JP, Dissanayake VU, Briggs AR, Milic MR, Gee NS (1998) Isolation of the [3H] gabapentin-binding protein/alpha 2 delta Ca2+ channel subunit from porcine brain: development of a radioligand binding assay for alpha 2 delta subunits using [3H]leucine. Anal Biochem 255: 236-243.

33 Marchler-Bauer A, Derbyshire MK, Gonzales NR, Lu S, Chitsaz F, et al. (2015) CDD: NCBI's conserved domain database. Nucleic Acids Res 43: D222-D226.

34 Yang JY, Yan RX, Roy A, Xu D, Poisson J, et al. (2015) The I-TASSER Suite: protein structure and function prediction. Nature methods 12: 7-8.

35 Roy A, Kucukural A, Zhang Y (2010) I-TASSER: a unified platform for automated protein structure and function prediction. Nat Protoc 5: 725-738.

36 Zhang Y (2008) I-TASSER server for protein 3D structure prediction. BMC Bioinformatics 9: 40.

37 Gaudet R (2009) Divide and conquer: high resolution structural information on TRP channel fragments. J Gen Physiol 133: 231-237.

38 Song L, Espinoza-Fuenzalida IA, Etheridge S, Jones OT, Fitzgerald EM (2015) The R-Domain: Identification of an N-terminal Region of the alpha2delta -1 Subunit Which is Necessary and Sufficient for its Effects on $Ca_V2.2$ Calcium Currents. Curr Mol Pharmacol 8: 169-179.

39 Baynes BM, Wang DI, Trout BL (2005) Role of arginine in the stabilization of proteins against aggregation. Biochemistry 44: 4919-4925.

40 Tsumoto K,Umetsu M, Kumagai I, Ejima D, Philo JS, et al. (2004) Role of arginine in protein refolding, solubilization, and purification. Biotechnol Prog 20: 1301-1308.

41 Nothaft H, Szymanski CM (2010) Protein glycosylation in bacteria: sweeter than ever. Nat Rev Microbiol 8: 765-778.

42 Petoukhov MV, DI Svergun (2015) Ambiguity assessment of small-angle scattering curves from monodisperse systems. Acta crystallographica Section D, Biological crystallography 71: 1051-1058.

43 Hura GL, Menon AL, Hammel M, Rambo RP, Poole FL, et al. (2009) Robust, high-throughput solution structural analyses by small angle X-ray scattering (SAXS). Nature Methods 6: 606- 612.

44 Putnam CD, Hammel M, Hura GL, Tainer JA (2007) X-ray solution scattering (SAXS) combined with crystallography and computation: defining accurate macromolecular structures, conformations and assemblies in solution. Q Rev Biophys 40: 191-285.

45 Boldon L, Laliberte F, Liu L (2015) Review of the fundamental theories behind small angle X-ray scattering, molecular dynamics simulations, and relevant integrated application. Nano reviews 6: 25661.

46 Putnam DK, Lowe EW, Meiler J (2013) Reconstruction of SAXS Profiles from Protein Structures. Comput Struct Biotechnol J 8: e201308006.

47 dos Reis MA, Aparicio R, Zhang Y (2011) Improving Protein Template Recognition by Using Small-Angle X-Ray Scattering Profiles. Biophysical Journal 101: 2770-2781.

48 Svergun DI (1999) Restoring low resolution structure of biological macromolecules from solution scattering using simulated annealing (vol 76, pg 2879, 1999). Biophysical Journal 77: 2896-2896.

49 Konarev PV, Volkov VV, Sokolova AV, Koch MHJ, Svergun DI (2003) PRIMUS: a Windows PC-based system for small-angle scattering data analysis. J Appl Crystallogr 36: 1277-1282.

50 Svergun D, Barberato C, Koch MHJ (1995) CRYSOL - A program to evaluate x-ray solution scattering of biological macromolecules from atomic coordinates. J Appl Crystallogr 28: 768-773.

51 Petoukhov MV, Svergun DI (2015) Ambiguity assessment of small-angle scattering curves from monodisperse systems. Acta Crystallogr 71: 1051-1058.

52 Upadhyay AA, Fleetwood AD, Adebali O, Finn RD, Zhulin IB (2016) Cache Domains That are Homologous to, but Different from PAS Domains Comprise the Largest Superfamily of Extracellular Sensors in Prokaryotes. Plos Comput Biol 12.